Journal of Renewable Energies

Revue des Energies Renouvelables

journal home page : https://revue.cder.dz/index.php/rer

New designs of turbulence promoters to use in saltwater purification processes

Mounir Amokrane [a,b,*], Djamel Sadaoui [b]

[a] *Département de Génie Mécanique, Faculté de Génie de la Construction, Université Mouloud Mammeri de Tizi Ouzou, Tizi Ouzou, Algérie*

[b] *Laboratoire de Mécanique Matériaux et Energétique (L2ME) Université de Bejaia, Bejaia, Algérie*

** Corresponding author, E-mail address: mounir139@live.fr*

Tel.: +213542846810

Abstract

This paper describes a two-dimensional computational fluid dynamics (CFD) model of flow with mass transfer to simulate a membrane separation system. The fluid domain comprises two reverse osmosis (RO) membranes and is fitted with different wavy inserts that act as turbulence promoters. Four types of insert designs were evaluated in terms of salt deposition on the membranes, permeate flux, axial pressure drop in the channel, and plots of the Sherwood number against the Power number. According to numerical simulations, under the operating conditions of this investigation, the proposed designs generate better results than commercial designs. The gain in pure water flux achieves up to 2%, and salt deposition on the membrane surface is reduced by ~5% than the commercial Zigzag spacer arrangement.

Keywords: Reverse osmosis, CFD, Desalination, Concentration polarization

1. Introduction

Spiral Wound Membrane (SWM) modules are used in the reverse osmosis process to retain salts contained in seawater and thus produce potable water. SWM modules are usually composed of dense membranes wrapped around a hollow tube that collects pure water flux [1]. A mesh layer is introduced between successive membranes and acts as a turbulence promoter, resulting in improved process and increased energy losses inside the module [2]. The simulation of the flow field with mass transfer within commercial SWM modules [3, 4] or new designs of RO systems [5-7] have been treated by many researchers. According to studies, the spatial arrangement and the shape of obstacles impact the separation process. In this paper, a two-dimensional CFD model is used to simulate a channel bounded by two RO

membranes and fitted with four types of wavy inserts. Thus, this study aims to evaluate the influence of these new shapes of inserts on the separation process and can be considered as an extension of our previous study [8].

2. Material and methods

2.1 Geometry

Figure 1 (a) shows the channel equipped with an undulated insert (Design 1) [8], while Figure 1 (b) shows the geometrical details of the inserts. It is important to note that the total length of the channel is L = 90 mm and, its height is H = 2 m. The distance between the insert and the inlet and outlet of the channel is 5 mm and 10 mm, respectively.

a)

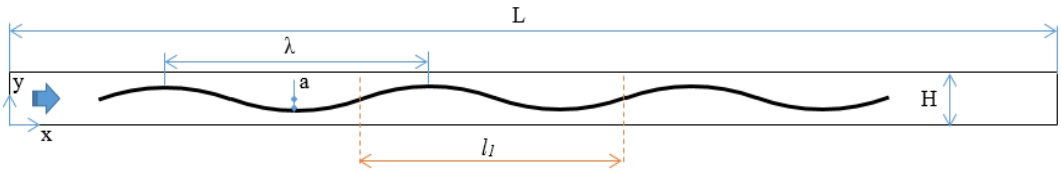

b)

Design 1 (a = 0.5 mm, λ = 24 mm)

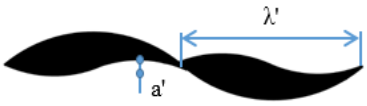

Design 2 (a = 0.5 mm, λ = 24 mm, a'= 0.2 mm and λ' = 12 mm)

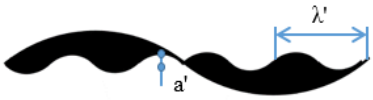

Design 3 (a = 0.5 mm, λ = 24 mm, a'= 0.2 mm, λ' = 6 mm)

Design 4 (a = 0.5 mm, λ = 24 mm, *d* = 1 mm)

Fig 1. Schematic representation of the channel (a) and insert designs (b).

2.1 Governing equations

The following dimensionless equations are used to describe the circulation of the saltwater inside the channels shown above:

$$\nabla.(\rho\mathbf{V})=0 \tag{1}$$

$$\nabla.(\rho\mathbf{VV})=\nabla.[\mu(\nabla\mathbf{V}+\nabla\mathbf{V}^{\mathbf{T}})]-\nabla p \tag{2}$$

$$\nabla.(\rho \mathbf{V} m_A)=\nabla.(\rho D_{AB} \nabla m_A) \quad (3)$$

Here, the flow is assumed to be isothermal, steady-state, laminar, and incompressible. Gravity, viscous dissipation, and compressibility are not considered in the model.

In the above equations ρ, μ, **V** and p, are the density, dynamic viscosity, velocity field and pressure while m_A and D_{AB} are the salt mass fraction and the binary diffusion coefficient of the solute A in the solvent B, respectively.

2.2 Boundary conditions

The saltwater flowing within the simulated channels is a mixture of pure water and salt (NaCl solution), and its physicochemical properties (ρ, μ, DAB) vary according to the empirical relations of Geraldes et al. [9].

The boundary conditions are as follows:

At the channel inlet ($0 \leq y \leq H; x = 0$):

$$u = u_0 \ (100 \leq Re_{ch} (Re_{ch} = \rho u_0 H/\mu) \ ) \leq 380 \ ); v = 0; \ m_A = m_{A0} = 0.02 \ \frac{kg}{kg} \quad (4)$$

At the channel outlet ($0 \leq y \leq H; x = L$):

$$\frac{\partial u}{\partial y}=0; \ \frac{\partial v}{\partial y}=0; \ \frac{\partial m_A}{\partial y}=0 \quad (5)$$

Inserts:

$$\frac{\partial u}{\partial y}=0; \ \frac{\partial v}{\partial y}=0; \ \frac{\partial m_A}{\partial y}=0 \quad (6)$$

Upper and lower membranes ($0 \leq x \leq L; y = 0 \text{ and } y = H$):

$$\pm J_v = \pm \frac{1}{R_m \mu_w} (\Delta P - \Delta \pi) \quad (7)$$

$$J_v \, R \, m_A = -D_{AB} (\partial m_A / \partial y) \quad (8)$$

In the previous equations, μ_w is the dynamic viscosity of the pure water, R_m is the membrane resistance (1.562×10^{14} m^{-1}); ΔP is the transmembrane pressure ($8.103 \ 10^5$ Pa); R is the intrinsic membrane rejection (0.99) and J_v is the permeate flux.

2.3 Solution methods

The Navier-Stokes and solute equations coupled with the boundary conditions are solved using the iterative Finite Volume Method (CFD code Fluent 6.3). Depending on the geometry of the insert, the fluid domains are meshed using non-uniform mesh grids containing between 51069 and 54043 nodes. Furthermore, the mesh is refined near membrane walls where the

concentration polarization (CP) layer forms. Spatial discretization of second-order UPWIND is used for pressure, momentum, and scalar equations, while the SIMPLE scheme is used for pressure-velocity coupling. A criterion of convergence of 10^{-8} is chosen to check the accuracy of the results.

3. Results and discussion

The streamlines obtained at Re_{ch} = 380 between the cross-sections (x = 30 mm and 42 mm) are shown in Fig. 2. Regardless of the insert design, the flow remains laminar without disturbance, in contrast to the commercial submerged spacer configuration [2]. Designs 1, 2, and 3 accelerate the flow without generating recirculations. While for Design 4, recirculations appear upstream and downstream of the circular shape.

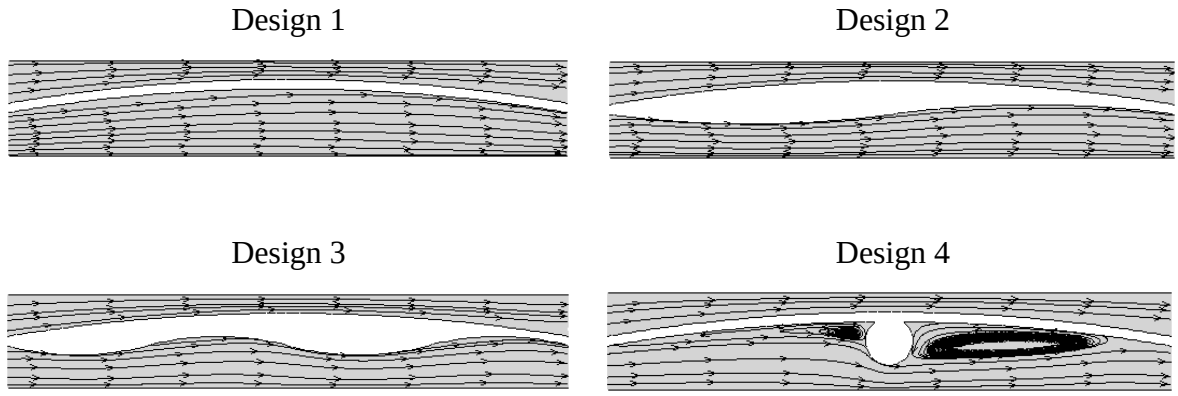

Fig 2. Streamlines obtained with different insert designs at Re_{ch} = 380

The evolution of the mass fraction (m_{Am}) recorded over the lower membrane surface (l_1) at Re_{ch} = 380 is shown in Fig. 3. As expected, the addition of sub-waves (Designs 2, 3) or a spacer (Design 4) to the crest of the wavy insert further disturbs the CP layer and hence reduces the salt deposition on the membrane surface.

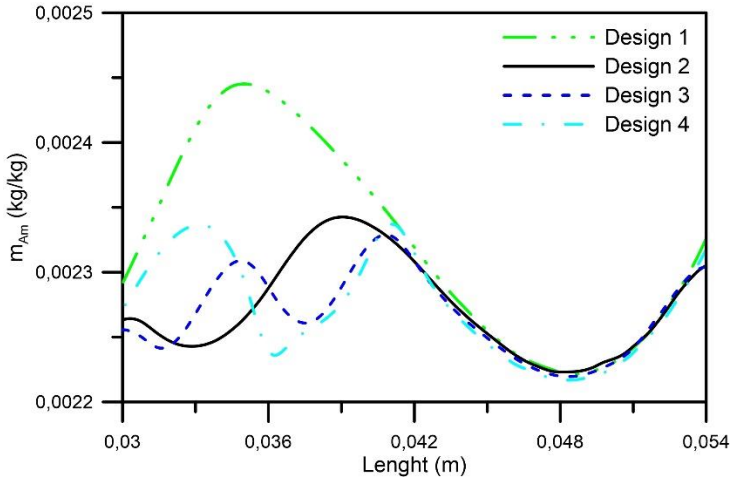

Fig 3. Salt mass fraction profiles along the lower membrane surface 'l_1' at Re_{ch} = 380.

The space-averaged values of the salt mass fraction (a) and permeate flux (b) computed along the lower membrane (l_1) versus the Reynolds number are shown in Fig. 4. Design 1 records the highest salt accumulation on the membrane surface and the lowest permeate flux compared to the other designs. It is worth noting that the four designs of interest outperform the commercial Zigzag spacer arrangement.

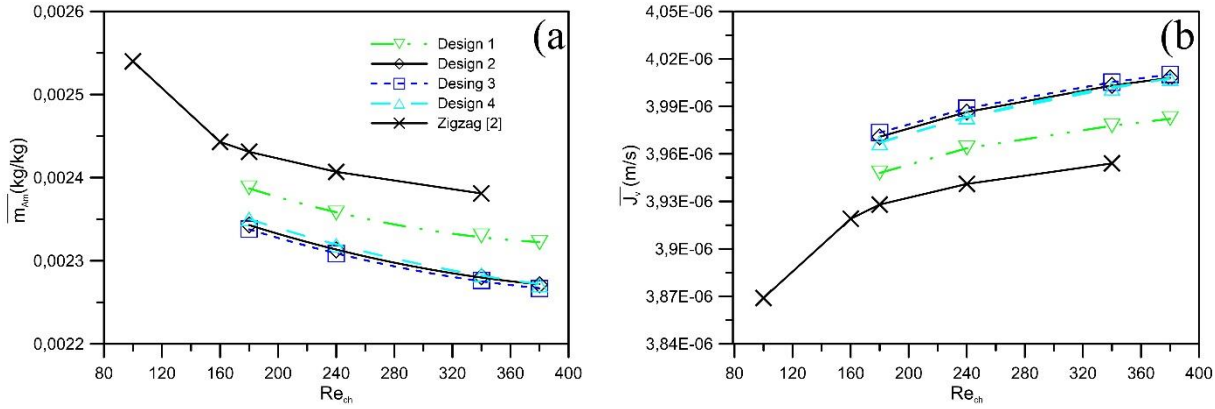

Fig 4. Space-averaged salt mass fraction (a) and permeation flux (b) as a function of the Reynolds number

Fig. 5 (a) shows the pressure drop per unit of length against the Reynolds number, whereas Fig. 5 (b) shows the overall Sherwood number ($Sh = k.H/D_{AB}$) against the Reynolds number. Design 1 records the lowest pressure drop than the other designs (e.g., it generates 13% to 16% fewer losses than Design 4). Indeed, the wavy insert has a low contact surface, resulting in reduced drag. Design 3 records the highest values of the Sherwood number compared to other designs, and the gain is about 12% to 15% compared to Design 1.

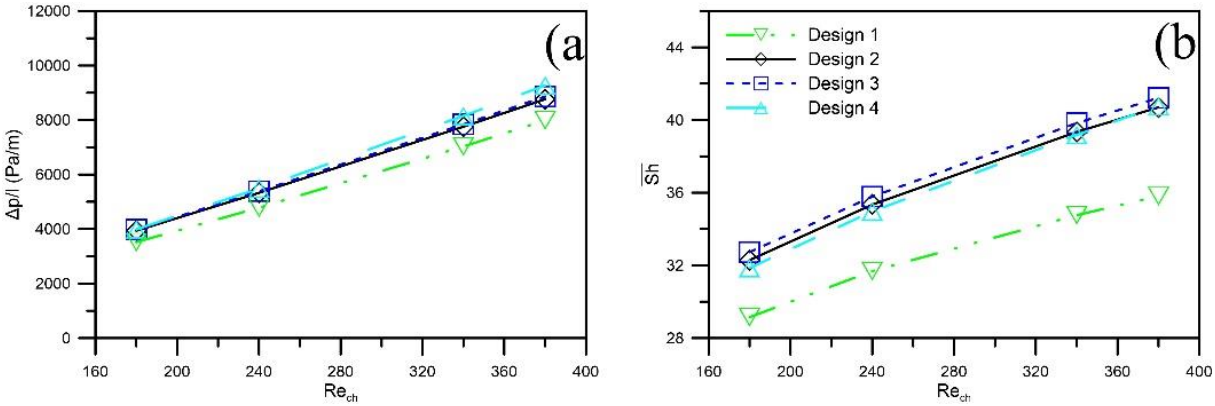

Fig 5. Pressure drop per unit length (a) and Sherwood number (b) as a function of the Reynolds number

The Sherwood number is plotted against the Power number ($Pn = \overline{f}\,Re_{ch}^3$), as shown in Fig. 6. Here, it is found that the Design 1 records the poorest ratio between mass transfer and energy consumption than other designs. Meanwhile, Designs 2, 3, and 4 record a close performance.

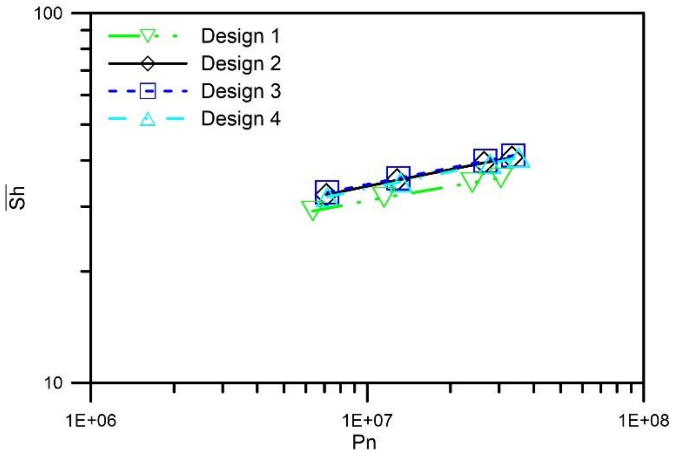

Fig 6. Sherwood number as a function of the Power number

4. Conclusions

This paper deals with a two-dimensional flow of NaCl aqueous solution inside a channel bounded by two RO membranes and fitted with different designs of inserts. Simulations were performed for different Reynolds numbers and a constant value of the inlet mass fraction. According to CFD calculations, Designs 2, 3, and 4 generate close performance but are superior to Design 1. In other words, wavy inserts equipped with sub-waves or spacers generate lower salt deposition on membranes and higher permeate flux than Design 1. Overall, results confirm the beneficial use of wavy-shaped inserts in membrane applications. However, experimental investigations are recommended to support the numerical results of this study.

5. References

[1] Haidari AH, Heijman SGJ, van der Meer WGJ, Effect of spacer configuration on hydraulic conditions using PIV, Sep Purif Technol 2018;199:9-19. https://doi.org/10.1016/j.seppur.2018.01.022

[2] Amokrane M, Sadaoui D, Koutsou CP, Karabelas AJ, Dudeck M, A study of flow field and concentration polarization evolution in membrane channels with two-dimensional spacers during water desalination, J Membr Sci 2015;477:139–150. https://doi.org/10.1016/j.memsci.2014.11.029

[3] Karabelas AJ, Kostoglou K, Koutsou CP, Modeling of spiral wound membrane desalination modules and plants – review and research priorities, Desalination 2015;365: 165-186. https://doi.org/10.1016/j.desal.2014.10.002

[4] Haidari AH, Heijman SGJ, Van der Meer WGJ, Optimal design of spacers in reverse osmosis. Sep Purif Technol 2018;192:441-456. https://doi.org/10.1016/j.seppur.2017.10.042

[5] Ranade VV, Kumar A, Fluid dynamics of spacer filled rectangular and curvilinear channels, J Membr Sci 2006; 271:1–15. https://doi.org/10.1016/j.memsci.2005.07.013

[6] Guillen G, Hoek EMV, Modeling the impacts of feed spacer geometry on reverse osmosis and nanofiltration processes, *Chem Eng J* 2009;149:221–231. https://doi.org/10.1016/j.cej.2008.10.030

[7] Amokrane M, Sadaoui D, Improving the reverse osmosis desalination system with tilted oval spacers in a zigzag configuration, Desal Water Treat 2021;211:359–368. https://doi.org/10.5004/dwt.2021.26811

[8] Geraldes V, Semião V, Pinho MN, Numerical modelling of mass transfer in slits with semi-permeable membrane walls, Eng Comput;2000: 17:192-217. https://doi.org/10.1108/02644400010324857

[9] Amokrane M, Sadaoui D, Undulated insert for boosting desalination efficiency in membrane systems, Braz Journal of Chem Eng 2021, https://doi.org/10.1007/s43153-021-00151-0